ACS APPLIED MATERIALS & INTERFACES

Research Article

Cite This: ACS Appl. Mater. Interfaces 2019, 11, 7472−7478

www.acsami.org

Rapid and Efficient Coacervate Extraction of Cationic Industrial Dyes from Wastewater

Benjamin Valley, Benxin Jing, Manuela Ferreira, and Yingxi Zhu*

Department of Chemical Engineering and Materials Science, Wayne State University, Detroit, Michigan 48202, United States

Supporting Information

ABSTRACT: Effluent wastewater containing dyes from textile, paint, and various other industrial wastes have long posed environmental damage. Functional nanomaterials offer new opportunities to treat these effluent wastes in an unprecedentedly rapid and efficient fashion due to their large surface area-to-volume ratio. In this work, we explore a new approach of wastewater treatment using macroionic coacervate complexes formed with zwitterionic polyampholytes and anionic inorganic polyoxometalate (POM) nanoclusters to extract methylene blue (MB) dye as well as other cationic industrial dyes from model wastewater. Biphasic organic−inorganic macroion complexes are designed to produce a small volume of coacervate adsorbents of high density and viscoelasticity, in contrast to a large volume of supernatant solution for rapid and efficient dye removal. The efficiency of coacervate extraction is characterized by the adsorption isotherm and maximum MB uptake capacity against the concentrations of polyampholyte, POM, and LiCl salt using UV−vis spectrophotometry to optimize the coacervate formation conditions. Our macroionic coacervate complexes could reach nearly 99% removal efficiency for the model wastewater samples of varied MB concentration in <1 min. The extraction capacity up to ∼400 mg/g far surpasses the dye extraction efficiency of widely used activated carbon adsorbents. We also explore the regeneration of coacervate complexes containing high concentration of extracted MB by a simple Fenton oxidation process to bleach coacervate complexes for repeated POM usage, which shows similar MB extraction efficiency after regeneration. Hence, coacervate extraction based upon spontaneous liquid−liquid separating complexation between polyzwitterions and POMs is demonstrated as a rapid, efficient, and sustainable method for industrial dye wastewater treatment. In perspective, coacervate extraction could advantageously possess dual processing options in separation industry through either membrane fabrication or use directly in mixer-settlers.

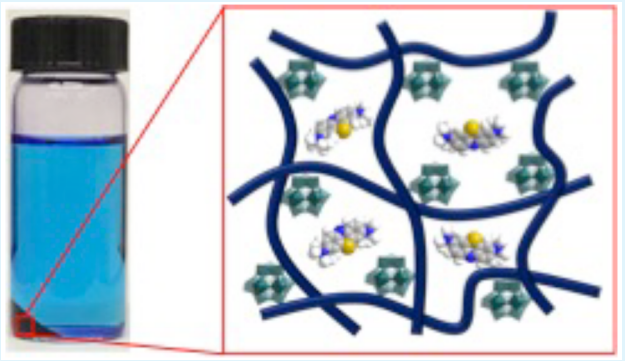

KEYWORDS: *coacervate extraction, wastewater treatment, industrial dye extraction, polymer−polyoxometalate coacervate complexes, coacervate regeneration*

1. INTRODUCTION

Synthetic dyes are used in a wide variety of industrial products and processes including textiles, paint, food, pharmaceuticals, cosmetics, and thermoplastic materials. Over 10000 different dyes are used industrially,[1] among which the textile industry as one of the primary dye consumers and polluters could discharge ∼200000 tons of dye-related wastes annually.[2,3] Dye-containing wastewater poses significant environmental threats due to its large volume generated and the effluents' harmful compositions,[4] the latter of which could result in oxygen deficiency and pose mutagenic properties. Hence, rapid and efficient dye removal methods and materials are always highly desired. Up to the present, the commonly adopted industrial approach for industrial dye removal is based upon activated carbons as sorbents because of their high surface area, mesoporous structure, and high surface reactivity.[5,6] With the rapid development of nanomaterials in past decades, many nanostructured sorbents, including clays and organoclays,[7] zeolite,[8] Fe_3O_4,[9] pentiptycene-based porous polymer network,[10] graphene and graphene oxide,[11,12] porous activated carbon of ultrahigh surface area,[13] and carbon nanotube,[14] have been explored for the remediation of dye containing effluents mainly due to their large surface areas or active sites.[15] However, it remains a grand challenge to improve the price-to-performance ratio of these nanomaterials to practically extend their applications for wastewater treatment. For example, a dilemma in the dispersion stability of nanomaterials in aqueous media is encountered: higher dispersion stability to achieve higher surface area-to-volume ratio is always desired for better adsorption performance of industrial dyes, yet it conversely increases the post-treatment cost such as recollecting, recycling, and regeneration of sorbents regardless of the cost of these raw nanomaterials. An efficient and environmentally and economically sustainable approach to remove

Received: December 11, 2018
Accepted: January 28, 2019
Published: January 28, 2019

DOI: 10.1021/acsami.8b21674
ACS Appl. Mater. Interfaces 2019, 11, 7472−7478

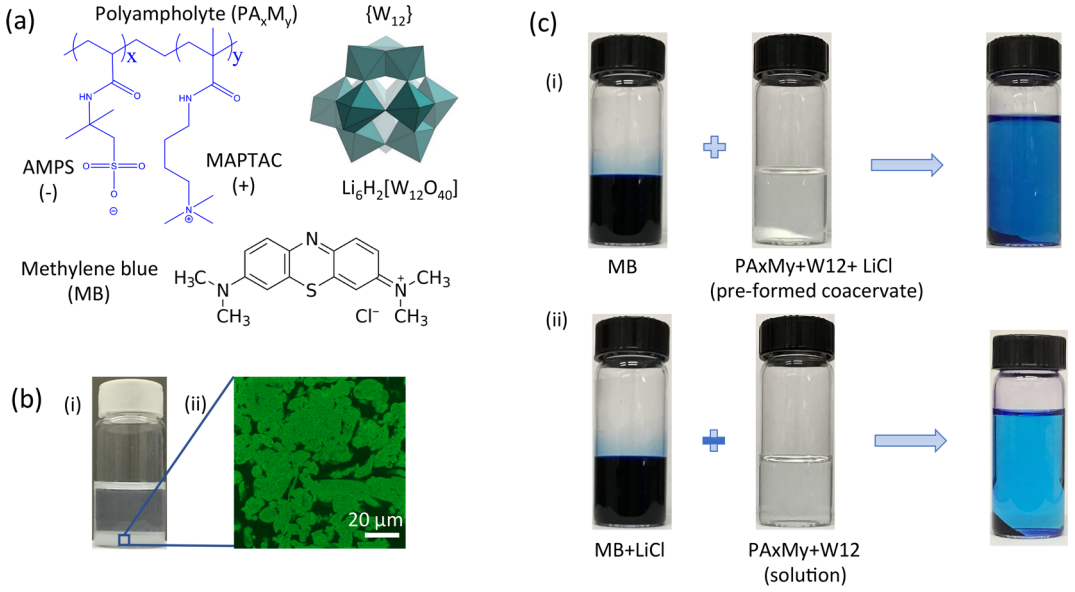

Figure 1. (a) Molecular structures of polyampholyte, P((AMPS)$_x$-*co*-(MAPTAC)$_y$) (PA_xM_y), lithium metatungstate, {W_{12}}, and cationic MB dye. (b) Digital photograph and fluorescent micrograph (of 100 μm × 100 μm) of $PA_{45}M_{55}$-{W_{12}}(200%) coacervate complex formed in aqueous solution added with 0.4 M LiCl in (i) and (ii), respectively, where FITC-labeled PA_xM_y is added before coacervate complexation in (ii). (c) Two typical processes of MB extraction by (i) mixing 10 mL of 0.4 g/L MB aqueous solution with 10 mL of preformed PA_xM_y-{W_{12}}(200%) (50 mg dry powder) coacervate complexes in 0.8 M LiCl aqueous solution and (ii) mixing 10 mL of 0.4 g/L MB in 0.8 M LiCl aqueous solution with salt-free PA_xM_y-{W_{12}} (200%) (50 mg of dry powder) aqueous solution. Clearly, both processes exhibit similar MB extraction performance.

industrial dye from vast amounts of wastewater remains in high demand.

In this work, we report a new and facile approach to rapidly and efficiently remove cationic dyes from wastewater by hybrid organic−inorganic macroionic coacervate complexes. Coacervate complexes are aqueous liquid−liquid phase separating systems, which exist commonly in charged polymers and biopolymers and contain one polymer-rich dense coacervate phase and the other polymer-poor supernatant phase. They have been used for the extraction and recovery of cells, proteins and enzymes, RNAs, and other biomasses.[16] Coacervate extraction could be developed as a promising, simple, and environmental friendly alternative to the conventional treatment of dye-containing wastewater.[17] However, the high volume fraction of conventional dense polymer coacervates and their low viscosity and density in close proximity to those of water make it difficult to rapidly and economically recover coacervate adsorbents from wastewater for repeated usage. Alternatively, we have recently explored hybrid coacervate complexation between inorganic polyanionic polyoxometalate (POM) nanoclusters and zwitterionic polymers in salted aqueous solution.[18] Such hybrid organic−inorganic macroionic complexation in salted solution could yield a gel-like dense coacervate phase in low volume fraction, whose density and viscoelasticity are modified to be significantly higher than those of supernatant aqueous solutions to facilitate rapid liquid−liquid separation by considerable density mismatch and enhanced mechanical strength for long-term durability.[18−20]

Specifically, in this work we explore the coacervate absorbents formed with metatungstate POM, $Li_6H_2W_{12}O_{40}\cdot xH_2O$ ({W_{12}}) of 0.8 nm diameter and bearing eight dissociable negative charges, and biocompatible zwitterionic polyampholyte copolymers composed of negatively charged 2-acrylamido-2-methyl-1-propanesulfonic acid (AMPS) and positively charged [3-(methacryloylamino)propyl]trimethylammonium chloride (MAPTAC) monomers, as their molecular structures are schematically displayed in Figure 1a. It is noted that as the density of {W_{12}} aqueous solution could be up to 2.95 g/cm^3, thereby {W_{12}} solution has been widely used as a thermally stable, economical, and safe heavy liquid for separations based on density mismatch.[21] Hence, it would also be much easier to separate {W_{12}}-based hybrid coacervate complexes than conventional polymer coacervate ones from supernatant solution. We evaluate the coacervate extraction performance by using methylene blue (MB) as a model cationic dye waste, while other cationic industrial dyes such as malachite green (MG) are also tested for the general applicability of coacervate extraction process. MB is a highly stable thiazine dye and widely used in the textile, medical, and printing industries, yet overexposure to it could conversely cause cardiac arrhythmias, coronary vasoconstriction, and decreased cardiac output among many adverse symptoms.[22] We choose MB as a model ionic waste also because of its high solubility in salted aqueous solutions and strong stability and resistance to decomposition in comparison to other cationic dyes. Here we examine the coacervate extraction of MB dye against net positively charged and net neutral polyampholytes, {W_{12}}-to-polyampholyte molar ratio, and MB dye concentration to determine the optimal formulation parameters of coacervate absorbents for best MB removal efficiency. To understand the mechanism of coacervate extraction, we determine the adsorption isotherm of MB dye in {W_{12}}-polyampholyte coacervate complexes of varied formulation conditions. The regeneration of coacervate adsorbents after industrial dye wastewater treatment is also tested for their potential impact on environmental sustainability.

2. EXPERIMENTAL SECTION

2.1. Materials. AMPS and MAPTAC monomers used for the synthesis of polyampholytes were purchased from Sigma-Aldrich and used directly. The synthesis procedure of polyampholytes by random

DOI: 10.1021/acsami.8b21674
ACS Appl. Mater. Interfaces 2019, 11, 7472−7478

free radical copolymerization is detailed elsewhere, for which AMPS monomer was neutralized by sodium hydroxide before polymerization.[20] The resulting copolymer, poly((AMPS)$_x$-*co*-(MAPMAC)$_y$), is abbreviated as PA$_x$M$_y$, where *x*:*y* is the feeding monomer molar ratio of m_{AMPS}:m_{MAPTAC}. In this work we examine PA$_{45}$M$_{55}$ and PA$_{50}$M$_{50}$ corresponding to *x*:*y* = 45:55 and 50:50, respectively. PA$_{45}$M$_{55}$ and PA$_{50}$M$_{50}$ show the respective electric potential ζ = 31.0 and 4.0 mV in aqueous solutions of LiCl concentration over the 0.03−0.1 M range by UV−vis spectrophotometric titration with a copolymerized pH indicator,[18,20] indicating that they are approximately net positively charged and net neutral in LiCl aqueous solution, respectively.

Industrial cationic dyes, methylene blue (MB), and anhydrous iron chloride ($FeCl_3$) were both purchased from Fisher Scientific and used directly. LiCl, hydrogen peroxide (H_2O_2), and other industrial cationic dyes, MG, and two industrial anionic dyes, acid black 1 (AB1) and acid red 27 (AR27), were all purchased from Sigma-Aldrich and used directly. An aqueous solution of {W$_{12}$} nanocluster was purchased from LMT Liquid and freeze-dried (Labconco Freezone 4.5 freeze-dryer) prior to use. All aqueous solutions were prepared with water purified by Barnstead Smart2Pure.

2.2. Preparation of PA$_x$M$_y$-{W$_{12}$} Coacervate Adsorbents. PA$_x$M$_y$ can dissolve in {W$_{12}$} or simple salt added aqueous solutions,[20] similar to many other zwitterionic polymers due to the antipolyelectrolyte effect.[18,19] The mixture of PA$_x$M$_y$ and {W$_{12}$} at certain concentration ranges in salted aqueous solutions could spontaneously separate into two liquid phases with one dense polymer/POM-rich coacervate phase and the other polymer/POM-poor supernatant phase.[20] To simplify the extraction procedure for dye removal, the mixture of PA$_x$M$_y$ and {W$_{12}$} in water of varied {W$_{12}$}-to-PA$_x$M$_y$ weight ratio, $w_{\{w12\}}/w_{PAxMy}$, was first freeze-dried to obtain powder-like samples. Subsequently, the powder-like complexes were added to LiCl aqueous solution to obtain small volumes of biphasic coacervate complexes as shown in Figure 1b. In this work, coacervate adsorbents obtained at $w_{\{w12\}}/w_{PAxMy}$ = 84% and 169%, corresponding to the molar ratio of {W$_{12}$} total charges to PA$_x$M$_y$ monomers at 100% and 200%, respectively, are investigated and designated as PA$_x$M$_y$-{W$_{12}$}(100%) and PA$_x$M$_y$-{W$_{12}$}(200%).

2.3. Quantification of Dye Extraction Efficiency. *Adsorption Kinetics.* To determine the adsorption kinetics, dry PA$_x$M$_y$-{W$_{12}$}-(100%) of mass amount, w_c = 36 mg and PA$_x$M$_y$-{W$_{12}$}(200%) of w_c = 50 mg were used. To enable the time-dependent dye adsorption measurement, we start with dispersing dry powder-like coacervate adsorbents in 200 μL of 0.4 M LiCl aqueous solution in disposable plastic cuvettes and centrifuged for 5 min at 3000 rpm to form white dense coacervate complexes. Subsequently, 3.8 mL of MB solution of initial concentration C_i = 0.008 g/L was added to the biphasic coacervate complexes. UV−vis spectra of MB in the supernatant solution at a fixed wavelength of 663 nm were acquired every 5 s immediately after adding MB solution to the coacervate complexes by UV−vis spectrophotometry (V-630, JASCO) to determine the residual MB concentration, C_t. The adsorption q_t (unit: mg/g) was calculated as

$$q_t = \frac{V(C_i - C_t)}{w_c} \quad (1)$$

where *V* is the total volume (= 4.0 mL) of the MB solution.

Adsorption Isotherm. Adsorption isotherm experiments were conducted at 25.0 ± 1.0 °C with w_c = 36 mg of PA$_x$M$_y$-{W$_{12}$}(100%) and 50 mg of PA$_x$M$_y$-{W$_{12}$}(200%) complexes. For these experiments, the coacervate complexes were prepared by first dispersing dry PA$_x$M$_y$-{W$_{12}$} complexes in 1.0 mL of LiCl aqueous solution with C_i = 0.4−0.7 M and then adding 39 mL of aqueous solution containing MB of various C_i = 0.008−0.4 g/L and LiCl of the same concentration. The entire mixtures were stirred for 2 h to allow thorough mixing and subsequently stood for 12 h before being centrifuged to collect the supernatant phase. The dye concentration in the supernatant solution was determined to be the equilibrium adsorption concentration, C_e (unit: mg/L), by UV−vis spectrophotometry. Thus, the equilibrium adsorption capacity, q_e (unit: mg/g), was calculated as

$$q_e = \frac{V(C_i - C_e)}{w_c} \quad (2)$$

where *V* is the total volume (= 40 mL) of the MB solution.

Maximum Adsorption Capacity. As the measured q_e−C_e relationship from the adsorption isotherm is neither linear nor exponential (see Figure 3), it is impossible to fit the curves by classical adsorption model to determine the maximum adsorption capacity, q_{max}.[23] To compare the coacervate extraction performance with other dye removal methods, continuous extraction was adopted to determine the maximum dye removal efficiency of coacervate complexes. Briefly, the isothermal adsorption with MB aqueous solution of C_i = 0.2 g/L added with 0.4 M LiCl was repeatedly measured with the same coacervate complexes until C_e/C_i approaches 10%. The reason to select $C_e/C_i \cong$ 10% was based on the observation that the MB removal efficiency became nearly constant at C_e/C_i < 10% with repeated measurements while it quickly decreased at C_e/C_i > 10%. The total amount of removed MB at C_e/C_i < 10% was used to calculate maximum adsorption capacity, q_{max}.

2.4. Dye Oxidation and Coacervate Adsorbent Regeneration. The well-known Fenton reagents were adopted to oxidize the dyes after coacervate extraction.[24] After the isothermal adsorption experiment, the dense coacervate complex was collected via centrifugation and redispersed in the mixture of 1.5 mL of water and 3.0 mL of 30 wt % H_2O_2 aqueous solution. Subsequently, 0.5 mL of 0.1 M $FeCl_3$ aqueous solution as the catalyst was added to the dense coacervate. After 10 min, the deep blue color of the coacervate suspension changes to brown. Finally, the yielding product after the removal of precipitation by centrifugation was added with PA$_x$M$_y$ and LiCl to maintain the original polymer and salt concentrations and complete the regeneration process. MB removal efficiency with the regenerated coacervate adsorbent was evaluated in the same process as described in section 2.3.

3. RESULTS AND DISCUSSION

To enable spontaneous liquid−liquid separating coacervate complexation for rapid and efficient removal of industrial dyes from wastewater, it is highly desired to produce a low volume fraction of dense coacervate phase with great contrast of its viscosity and density from those of supernatant solution. Instead of using oppositely charged polyelectrolytes to form conventional coacervate complexes, we use inorganic polyanionic {W$_{12}$} nanoclusters as one polymeric composite to form hybrid coacervate complexes with zwitterionic polyampholytes, resulting in significantly mismatched viscosity and density between the dense and supernatant phases to facilitate rapid separation post wastewater treatment.[18,19] The formation of PA$_x$M$_y$-{W$_{12}$} coacervate complexes in 0.4 M LiCl added aqueous solution is evidently exhibited in Figure 1b-i, where the bottom cloudy phase is the polyampholyte and {W$_{12}$}-rich phase and the top clear phase is the dilute supernatant phase. The biphasic coacervate complex is also confirmed by the presence of mobile supernatant droplets dispersed in fluorescent dense coacervate phase by using fluorescein labeled-PA$_x$M$_y$, as shown in Figure 1b-ii. The linear viscoelasticity of PA$_x$M$_y$-{W$_{12}$} dense coacervate complexes is enhanced by 2−5 orders of magnitude by the addition of {W$_{12}$} in comparison to that of PA$_x$M$_y$ solution of the same PA$_x$M$_y$ concentration as shown in Figure S1, which is also much higher than that of synthetic polyelectrolyte coacervate complexes reported in the literature[25] and could provide sufficient mechanical stability for long-term usage.

To examine the feasibility of coacervate extraction for wastewater treatment, we first mix the MB-containing model

DOI: 10.1021/acsami.8b21674
ACS Appl. Mater. Interfaces 2019, 11, 7472−7478

wastewater with PA_xM_y-$\{W_{12}\}$ coacervate complexes that are already formed in LiCl solution. Rapid adsorption of MB dye molecules onto coacervate adsorbents is observed as indicated by much darker blue color of the dense coacervate phase than the color of the supernatant phase, as shown in Figure 1c-i. To exclude the effect of mixing sequence on MB extraction, alternatively we mix the dark blue MB-LiCl solution with clear PA_xM_y and $\{W_{12}\}$ mixed salt-free aqueous solution. As indicated in Figure 1c-ii, upon mixing the two aqueous solutions, biphasic coacervate complex is immediately formed with dark blue dense coacervate complex in contrast to light blue supernatant solution. It is noted that for acquiring the photograph in Figure 1c-ii, the vials are centrifuged for 3 min at 3000 rpm to accelerate the coalescence of dense coacervate droplets containing extracted MB into a volume of dense coacervate complex and then the separation to the bottom of the vial by mismatched density from the supernatant solution. By UV−vis spectroscopic characterization as detailed below, we have determined that the residual MB concentration in the supernatant solution is 0.0022 g/L in Figure 1c-i versus 0.0012 g/L in Figure 1c-ii, corresponding to dye removal efficiency as high as 98.9% and 99.4%, respectively. Hence, we confirm that within experimental uncertainty the mixing sequence has negligible effect on dye extraction efficiency.

Similar extraction of cationic MG dye by PA_xM_y-$\{W_{12}\}$ coacervates is observed as shown in Figure S2a, confirming the general applicability of macroionic coacervate complex for the extraction of cationic dyes from wastewater. In sharp contrast, no apparent extraction of anionic dyes, AB1 and AR27, is observed with PA_xM_y-$\{W_{12}\}$ coacervates as shown in Figure S2. Hence, we speculate that the extraction of cationic dyes from wastewater by PA_xM_y-$\{W_{12}\}$ coacervate is resulted from strong electrostatic interaction between cationic dye molecules and anionic $\{W_{12}\}$ nanocluster as further investigated below.

To quantify the MB extraction efficiency, we determine the MB concentration in the supernatant solution after liquid−liquid separation by UV−vis spectroscopy. Control experiment shows that the intensity of the characteristic UV−vis absorbance peak of MB at the wavelength of 663 nm increases with MB concentration in aqueous solution, yielding a calibrated linear relationship of MB concentration against UV−vis characteristic peak intensity (see Figure S3). We also observe that the adsorption profile of MB in MB-$\{W_{12}\}$ mixed solution without PA_xM_y and LiCl is dramatically different from that of {W12}-free MB solution and supernatant solution after separation, strongly suggesting the binding of MB with $\{W_{12}\}$ due to electrostatic attraction (Figure S4). Conversely, no shift of the characteristic UV−vis peak in the supernatant solution after the removal of MB-adsorbed PA_xM_y-$\{W_{12}\}$ dense coacervate also suggests a negligible amount of $\{W_{12}\}$(Figure S4), which agrees well with the reported compositions in polyzwitterion-$\{W_{12}\}$ coacervate complexes.[18] Thus, the concentration of MB in the supernatant solution after coacervate extraction can be accurately determined to evaluate the efficiency of PA_xM_y-$\{W_{12}\}$ coacervate extraction.

Figure 2 shows the time-dependent change of MB amount in the supernatant solutions, which are collected at varied elapsed time upon the addition of MB wastewater to the continuous PA_xM_y-$\{W_{12}\}$ coacervate complexes of varied $w_{\{w12\}}/w_{PAxMy}$ on the bottom of the cuvette. Clearly, all the coacervate adsorbents used in this work can quickly extract cationic MB dyes from wastewater. The MB adsorption capacity, q_t, reaches the plateau in <60 s with all the coacervate absorbents of

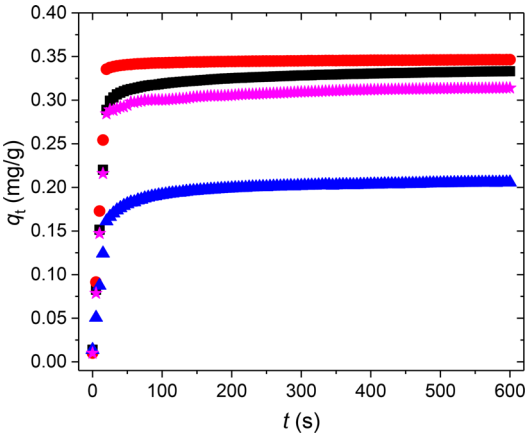

Figure 2. Time-dependent MB extraction capacity, q_t, of dry powder-like complexes of 36 mg $PA_{50}M_{50}$-$\{W_{12}\}$(100%) of (black squares), 36 mg $PA_{45}M_{55}$-$\{W_{12}\}$(100%) (blue triangles), 50 mg of $PA_{50}M_{50}$-$\{W_{12}\}$(200%) (red circles), and 50 mg and $PA_{45}M_{55}$-$\{W_{12}\}$(200%) (magenta stars) added to MB model wastewater of constant initial MB concentration of 0.008 g/L and LiCl concentration of 0.4 M.

PA_xM_y of varied net charge and $\{W_{12}\}$ content as shown in Figure 2. It is noted that the results shown in Figure 2 may reflect the kinetics of MB uptake by the interfacial layers of tens to hundreds micrometers thick in the top coacervate complex region, yet such rapid dye extraction occurs with the entire coacervate systems considering the size of coacervate droplets in Figure 1c is in the approximate, or smaller than, hundreds of micrometers scale. Most importantly, we contribute the fast extraction of MB by coacervate adsorbents to the liquid nature of coacervate adsorbents in the biphasic complex, where the diffusion of dyes in gel-like coacervate adsorbents is expected to be much faster than that in commonly used solid sorbents.

Next, we examine the adsorption isotherm of MB dye with PA_xM_y-$\{W_{12}\}$ coacervate complexes as shown in Figure 3. The measured equilibrium adsorption capacity, q_e, of PA_xM_y-$\{W_{12}\}$ complexes of different PA_xM_y polymers and $\{W_{12}\}$-to-PA_xM_y concentration ratio is plotted against MB equilibrium concentration, C_e, logarithmically in Figure 3a. A nonlinear coacervate adsorption isotherm is observed, apparently distinct from classical adsorption isotherms. Neither the Langmuir isotherm model, based on monolayer physisorption, nor the Brunauer−Emmett−Teller (BET) model, based on multilayer physisorption, can be used to fit the MB adsorption isotherm well. We attribute it to the particularly liquid nature of coacervate adsorbent while widely used Langmuir and BET models are developed for solid sorbents. Also because of dye extraction using gel-like coacervate complexes, classical theories for simple liquid−liquid extraction also fail to be applied directly for coacervate extraction reported in this work. It is strongly hoped that advanced theory could emerge to mechanistically elucidate the coacervate extraction process for the removal of industrial cationic dyes from wastewater. Nevertheless, the observed increase of q_e with increased $\{W_{12}\}$ concentration in the coacervate suggests that the adsorption of MB on PA_xM_y-$\{W_{12}\}$ coacervate complex possibly occurs on the anionic sites of $\{W_{12}\}$ due to $\{W_{12}\}$-MB electrostatic attraction in aqueous solution.

In our previous work, we have found that salt can considerately shift the boundary of the phase diagram for polyzwitterion-$\{W_{12}\}$ coacervate complexation.[18] Here we also

DOI: 10.1021/acsami.8b21674
ACS Appl. Mater. Interfaces 2019, 11, 7472−7478

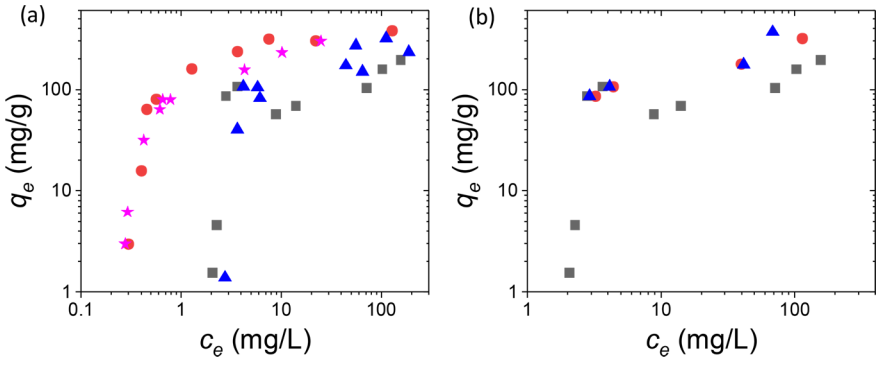

Figure 3. (a) MB adsorption isotherm, q_e, of 36 mg $PA_{50}M_{50}$-$\{W_{12}\}$(100%) (black squares), 36 mg $PA_{45}M_{55}$-$\{W_{12}\}$(100%) (blue triangles), 50 mg $PA_{50}M_{50}$-$\{W_{12}\}$(200%) (red circles), and 50 mg $PA_{45}M_{55}$-$\{W_{12}\}$(200%) (magenta stars) against equilibrium MB concentration, C_e, from model wastewater of initial MB concentration, C_i = 0.008−1.0 g/L, and constant 0.4 M LiCl. (b) MB adsorption isotherm, q_e, with 36 mg of $PA_{50}M_{50}$-$\{W_{12}\}$(100%) in model MB wastewater added with LiCl of 0.4 M (black squares), 0.5 M (red circles), and 0.7 M (blue triangles).

examine the effect of salt concentration in model wastewater on MB dye extraction efficiency. To simulate variable salinity conditions found in textile manufacturing wastewaters,[26] MB−LiCl aqueous solution of varied LiCl concentration at 0.4, 0.5, and 0.7 M are prepared to accommodate 36 mg $PA_{50}M_{50}$-$\{W_{12}\}$(100%). The q_e−C_e isotherm of MB adsorption $PA_{50}M_{50}$-$\{W_{12}\}$(100%) show strong dependence on LiCl concentration in Figure 3b. MB adsorption amount increases nearly 30% with increasing LiCl concentration from 0.4 to 0.7 M. We have excluded the screening effect as the Debye screening length change very little from 0.48 to 0.36 nm as increasing LiCl concentration in this work. Also, the volume of dense coacervates upon liquid−liquid phase separation decreases with increasing salt from 0.4 to 0.7 M. Thus, the salt enhanced efficiency of coacervate extraction of dyes might be resulted from the microstructural change of $PA_{50}M_{50}$-$\{W_{12}\}$ coacervate, in which the mesh size of gel-like polyzwitterion-$\{W_{12}\}$ coacervate could decrease with increasing LiCl concentration so as to further limit the mobility of trapped dyes.[18,19] These results strongly suggest the promise of coacervate adsorbents as a competitive wastewater treatment because they can sustain high effectiveness over a range of high salt concentration. The maximum adsorption capacity, q_{max}, cannot be obtained from the q_e−C_e isotherm due to the lack of a suitable model for liquid-based coacervate extraction; instead, we determine q_{max} from continuous MB removal using the same coacervate complex of fixed mass. Accordingly, optimal formulation parameters of PA_xM_y-$\{W_{12}\}$ coacervate adsorbents for the best MB extraction efficiency are determined based on q_{max}. In comparison of the measured q_{max} among four different PA_xM_y-$\{W_{12}\}$ coacervate adsorbents, $PA_{45}M_{55}$-$\{W_{12}\}$(200%) coacervate stands out to exhibit the highest q_{max} = 397.6 mg/g, as shown in Figure 4. The adsorption isotherm results shown in Figure 3 also indicate that PA_xM_y-$\{W_{12}\}$ (200%) coacervates outperform PA_xM_y-$\{W_{12}\}$(100%) ones. As combined, we rank the $PA_{45}M_{55}$-$\{W_{12}\}$(200%) coacervate complex exhibits the best MB extract efficiency because of the following considerations. As our results suggest that MB extraction is due to the electrostatic attraction between MB and $\{W_{12}\}$, apparently increasing $\{W_{12}\}$ content in the coacervates offers more adsorption sites for cationic MB. Additionally, $\{W_{12}\}$ polyanions can bind with net positively charged $PA_{45}M_{55}$ more strongly than net neutral $PA_{50}M_{50}$, resulting in higher content of $\{W_{12}\}$ in the coacervates. Furthermore, the resulting gel-like microstructure of $PA_{45}M_{55}$-$\{W_{12}\}$ (200%) bears smaller mesh

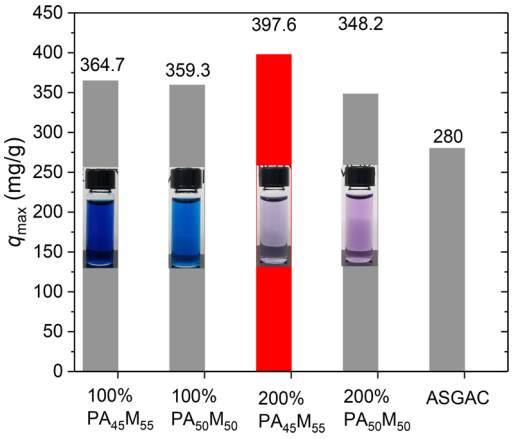

Figure 4. Maximum adsorption capacity, q_{max}, of four different coacervate complexes, $PA_{45}M_{55}$-$\{W_{12}\}$(100%), $PA_{50}M_{50}$-$\{W_{12}\}$-(100%), $PA_{45}M_{45}$-$\{W_{12}\}$(200%), and $PA_{50}M_{50}$-$\{W_{12}\}$(200%), in comparison to that reported of commercial adsorbent, AquaSorb 2000-granular coal-based activated carbon (ASGAC), for which 0.2 g/L MB aqueous solution added with 0.4 M LiCl is used for continuous extraction.

pore size approaching to the size of MB.[18,19] It should be also noted that despite the optimal design of $PA_{45}M_{55}$-$\{W_{12}\}$(200%) coacervate for the best MB extraction performance, the measured q_{max} of $PA_{45}M_{55}$-$\{W_{12}\}$ (100%) and $PA_{50}M_{50}$-$\{W_{12}\}$(200%) coacervates is merely ∼10% lower than that of $PA_{45}M_{55}$-$\{W_{12}\}$ (200%). Hence, all the PA_xM_y-$\{W_{12}\}$ coacervates exhibit much higher MB adsorption capacity (>350 mg/g) than the reported capacity of 280 mg/g for widely used commercial absorbent, AquaSorb 2000-granular coal-based activated carbon (ASGAC).[27]

Last but not the least, we examine the regeneration of coacervate−dye sludge post the extraction process. We have explored the Fenton process, which has become a common type of advanced oxidation processes used for post wastewater treatment,[24] to decompose extracted MB in dense coacervate and recover the expensive inorganic $\{W_{12}\}$ nanocluster. Fenton reagent, composed of hydrogen peroxide and ferrous ions, is known to be a rapid and nonselective oxidizer for organic materials. In comparison to enzyme-based mild decolorized methods,[28,29] Fenton reagent is much cheaper and oxidizes organic materials more thoroughly for practical application. In this work, the Fenton reagent containing 10.0 mM $FeCl_3$ and

DOI: 10.1021/acsami.8b21674
ACS Appl. Mater. Interfaces 2019, 11, 7472−7478

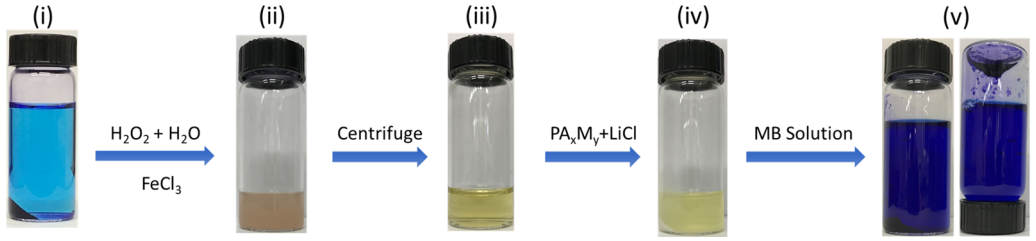

Figure 5. Photographic illustration of the regeneration process of MB-adsorbed $PA_{45}M_{55}$-{W_{12}} post wastewater treatment, which starts with (i) the blue biphasic coacervate complex (using the same formulation with Figure 1c), removing supernatant, adding the mixture 1.5 mL of water and 3.0 mL of 30 wt % H_2O_2 aqueous solution to redisperse the coacervate, and then adding 0.5 mL of 100 mM $FeCl_3$ aqueous solution followed by incubation for 10 min to oxidize the dye (ii). After removing any precipitation by centrifugation, {W_{12}} is recovered as a yellow solution (iii). Subsequently 0.93 mL 20.0 g/L $PA_{45}M_{55}$ in 0.1 M LiCl aqueous solution and 0.8 mL of 10.0 M LiCl aqueous solution were added to get the new coacervate complexes (iv) and complete the regeneration process. Finally, 10 mL of 0.4 g/L MB aqueous solution and 2.0 mL of water were added to (iv) to repeat MB extraction (v).

5.9 M H_2O_2 is imbedded into the coacervate adsorbents to regenerate {W_{12}} after the removal MB from model wastewater. Reaction is initiated by adding the Fenton reagent to coacervate phase. As shown in Figure 5, complete bleaching of coacervate adsorbent is achieved, showing nearly no apparent blue color in the dense coacervate phase while the yellow color is the color of Fe^{3+} ion remaining in water. Subsequently, we have retested the performance of bleached coacervate adsorbents with 0.2 g/L MB solution, where additional $PA_{45}M_{55}$ in LiCl aqueous solution is added to form coacervate complexes with regenerated {W_{12}}. Despite the difficulty in differentiating the color between the supernatant and coacervate phases after MB extraction, the deep blue color of the coacervate phase adhered to the bottom of the inverted vial as shown in the right-side photograph of Figure 5v clearly suggests the extraction of MB. UV−vis spectroscopic results shown in Figure S5 further verify that the MB removal efficiency using regenerated $PA_{45}M_{55}$-{W_{12}}(200%) coacervate adsorbents remains as high as 96.7%, slightly lower than the 99.4% removal efficiency using fresh coacervate samples. It is clearly indicated that recovered {W_{12}} nanoclusters survive from the oxidation process and can re-form coacervate complexes with comparable MB extraction efficiency after the bleaching process. For practical use, such dye removal performance for regenerated adsorbents is common and acceptable for a compromise of material saving and environmental sustainability.

4. CONCLUSIONS

In this work, we have demonstrated a highly efficient and rapid coacervate extraction process for the removal of industrial cationic dyes from wastewater using organic−inorganic macroionic coacervate adsorbents. Maximum MB adsorption onto the dense coacervate complexes is observed with $PA_{45}M_{55}$-{W_{12}}(200%), which is formed with net positively charged $PA_{45}M_{55}$ and {W_{12}} polyanion at {W_{12}} charge-to-PAM monomer molar ratio of 200%, at relatively low salt concentrations of 0.4 M. The measured maximum MB adsorption capacity approximates to 400 mg/g, far exceeding the performance of commonly used activated carbon sorbents. While extraction performance is strongly enhanced with increasing wastewater salinity, our coacervate adsorbents perform exceptionally better than several conventional wastewater treatment methods over all the tested salt concentrations. Additionally, coacervate extraction is demonstrated to be a much faster process than traditional heterogeneous adsorbents, where over 90% dye removal efficiency can be achieved in less than a minute upon mixing wastewater with coacervate adsorbent. Rapid adsorption kinetics is attributed to the liquid nature of coacervate adsorbents. Furthermore, doping coacervate adsorbents with the Fenton reagent can successfully recover inorganic {W_{12}} nanoclusters from MB-saturated coacervate adsorbents while simultaneously decomposing and decolorizing adsorbed dyes in the coacervate phase. The regenerated coacervate adsorbent exhibits comparable dye removal efficiency to the fresh one, demonstrating an environmentally sustainable nanomaterial and process for wastewater treatment. In perspective, thanks to the simplicity of the spontaneous coacervate complexation in aqueous solution, coacervate adsorbents can offer dual processing options through either membrane fabrication or direct use in mixer-settler and become an excellent choice for sustainable manufacturing processes using industrial waste mass exchange networks.

■ ASSOCIATED CONTENT

Supporting Information

The Supporting Information is available free of charge on the ACS Publications website at DOI: 10.1021/acsami.8b21674.

Experimental details and Figues S1−S5 (PDF)

■ AUTHOR INFORMATION

Corresponding Author

*(Y.Z.) E-mail yzhu3@wayne.edu.

ORCID

Benxin Jing: 0000-0002-8400-1937

Author Contributions

B.V. and B.J. equally contributed to this work.

Notes

The authors declare no competing financial interest.

■ ACKNOWLEDGMENTS

The authors are grateful for the financial support from the National Science Foundation (NSF DMR-1743041).

■ REFERENCES

(1) Gürses, A.; Açıkyıldız, M.; Güneş, K.; Gürses, M. S. Dyes and Pigments: Their Structure and Properties. In *Dyes and Pigments*; Springer International Publishing: Cham, 2016; pp 13−29.

(2) Chequer, F. M. D.; de Oliveira, G. A. R.; Ferraz, E. R. A.; Cardoso, J. C.; Zanoni, M. V. B.; de Oliveira, D. P. *Textile Dyes: Dyeing Process and Environmental Impact*; Tech Press: 2013.

DOI: 10.1021/acsami.8b21674
ACS Appl. Mater. Interfaces 2019, 11, 7472−7478

(3) Şen, S.; Demirer, G. N. Anaerobic treatment of real textile wastewater with a fluidized bed reactor. *Water Res.* **2003**, *37* (8), 1868−1878.
(4) Forgacs, E.; Cserháti, T.; Oros, G. Removal of synthetic dyes from wastewaters: a review. *Environ. Int.* **2004**, *30* (7), 953−971.
(5) Reife, A.; Freeman, H. S. *Carbon Adsorption of Dyes and Selected Intermediates*; John Wiley & Sons, Inc.: New York, 1996.
(6) Bansal, R. C.; Goyal, M. *Activated Carbon Adsorption*; CRC Press: Boca Raton, FL, 2005.
(7) Huang, P.; Kazlauciunas, A.; Menzel, R.; Lin, L. Determining the Mechanism and Efficiency of Industrial Dye Adsorption through Facile Structural Control of Organo-montmorillonite Adsorbents. *ACS Appl. Mater. Interfaces* **2017**, *9* (31), 26383−26391.
(8) Shaw, R.; Sharma, R.; Tiwari, S.; Tiwari, S. K. Surface Engineered Zeolite: An Active Interface for Rapid Adsorption and Degradation of Toxic Contaminants in Water. *ACS Appl. Mater. Interfaces* **2016**, *8* (19), 12520−12527.
(9) Dalvand, A.; Nabizadeh, R.; Reza Ganjali, M.; Khoobi, M.; Nazmara, S.; Hossein Mahvi, A. Modeling of Reactive Blue 19 azo dye removal from colored textile wastewater using L-arginine-functionalized Fe_3O_4 nanoparticles: Optimization, reusability, kinetic and equilibrium studies. *J. Magn. Magn. Mater.* **2016**, *404*, 179−189.
(10) Luo, S.; Zhang, Q.; Zhang, Y.; Weaver, K. P.; Phillip, W. A.; Guo, R. Facile Synthesis of a Pentiptycene-Based Highly Microporous Organic Polymer for Gas Storage and Water Treatment. *ACS Appl. Mater. Interfaces* **2018**, *10* (17), 15174−15182.
(11) Shen, Y.; Chen, B. Sulfonated Graphene Nanosheets as a Superb Adsorbent for Various Environmental Pollutants in Water. *Environ. Sci. Technol.* **2015**, *49* (12), 7364−7372.
(12) Liu, F.; Chung, S.; Oh, G.; Seo, T. S. Three-Dimensional Graphene Oxide Nanostructure for Fast and Efficient Water-Soluble Dye Removal. *ACS Appl. Mater. Interfaces* **2012**, *4* (2), 922−927.
(13) Javed, H.; Luong, D. X.; Lee, C.-G.; Zhang, D.; Tour, J. M.; Alvarez, P. J. J. Efficient removal of bisphenol-A by ultra-high surface area porous activated carbon derived from asphalt. *Carbon* **2018**, *140*, 441−448.
(14) Li, Y.; Du, Q.; Liu, T.; Peng, X.; Wang, J.; Sun, J.; Wang, Y.; Wu, S.; Wang, Z.; Xia, Y.; Xia, L. Comparative study of methylene blue dye adsorption onto activated carbon, graphene oxide, and carbon nanotubes. *Chem. Eng. Res. Des.* **2013**, *91* (2), 361−368.
(15) Qu, X.; Alvarez, P. J. J.; Li, Q. Applications of nanotechnology in water and wastewater treatment. *Water Res.* **2013**, *47* (12), 3931−3946.
(16) Iqbal, M.; Tao, Y.; Xie, S.; Zhu, Y.; Chen, D.; Wang, X.; Huang, L.; Peng, D.; Sattar, A.; Shabbir, M. A. B.; Hussain, H. I.; Ahmed, S.; Yuan, Z. Aqueous two-phase system (ATPS): an overview and advances in its applications. *Biol. Proced. Online* **2016**, *18* (1), 18.
(17) Melnyk, A.; Namieśnik, J.; Wolska, L. Theory and recent applications of coacervate-based extraction techniques. *TrAC, Trends Anal. Chem.* **2015**, *71*, 282−292.
(18) Jing, B.; Qiu, J.; Zhu, Y. Organic−inorganic macroion coacervate complexation. *Soft Matter* **2017**, *13* (28), 4881−4889.
(19) Jing, I. B. a. B.; Xu, D.; Wang, X.; Zhu, Y. Multi-Responsive, Critical Gel Behaviors of Polyzwitterion-Polyoxometalate Coacervate Complexes. *Macromolecules* **2018**, *51* (22), 9405−9411.
(20) Ferreira, M.; Jing, B.; Zhu, Y. Effect of Polymer Net Charge on Polyampholyte-Polyanion Coacervate Complexation, 2018.
(21) LMT Liquid, l Lithium Metatungstate(LMT) Heavy Liquid; https://www.lmtliquid.com/lmt-home.html.
(22) Ginimuge, P. R.; Jyothi, S. D. Methylene Blue: Revisited. *J. Anaesthesiol., Clin. Pharmacol.* **2010**, *26* (4), 517−520.
(23) Masel, R. I. *Principles of Adsorption and Reaction on Solid Surfaces*; John Wiley & Sons, Inc.: New York, 1996.
(24) Hardin, I. R. 8 - Chemical treatment of textile dye effluent. In *Environmental Aspects of Textile Dyeing*; Christie, R. M., Ed.; Woodhead Publishing: 2007; pp 191−211.
(25) Liu, Y.; Winter, H. H.; Perry, S. L. Linear viscoelasticity of complex coacervates. *Adv. Colloid Interface Sci.* **2017**, *239*, 46−60.
(26) Chapter 3: Methods of Applying Dyes to Textiles. In *Textile Science and Technology*; Vigo, T. L., Ed.; Elsevier: 1994; Vol. *11*, pp 112−192.
(27) He, X.; Male, K. B.; Nesterenko, P. N.; Brabazon, D.; Paull, B.; Luong, J. H. T. Adsorption and Desorption of Methylene Blue on Porous Carbon Monoliths and Nanocrystalline Cellulose. *ACS Appl. Mater. Interfaces* **2013**, *5* (17), 8796−8804.
(28) Ashrafi, S. D.; Rezaei, S.; Forootanfar, H.; Mahvi, A. H.; Faramarzi, M. A. The enzymatic decolorization and detoxification of synthetic dyes by the laccase from a soil-isolated ascomycete, Paraconiothyrium variabile. *Int. Biodeterior. Biodegrad.* **2013**, *85*, 173−181.
(29) Mirzadeh, S.-S.; Khezri, S.-M.; Rezaei, S.; Forootanfar, H.; Mahvi, A. H.; Faramarzi, M. A. Decolorization of two synthetic dyes using the purified laccase of Paraconiothyrium variabile immobilized on porous silica beads. *J. Environ. Health Sci. Eng.* **2014**, *12* (1), 6−6.

DOI: 10.1021/acsami.8b21674
ACS Appl. Mater. Interfaces 2019, 11, 7472−7478